Network Operator Revenue Maximization in Dual Powered Green Cellular Networks

Ashutosh Balakrishnan, Swades De, and Li-Chun Wang

Abstract—Traffic-energy imbalance poses a major challenge on enabling of green-communication through dual-powered green networks, which are becoming increasingly attractive due to their cost efficiency and low carbon footprint. Dual-powered networks are prone to traffic-energy imbalance mainly due to spatio-temporal traffic variation and random solar energy harvest. Thus, it becomes imperative to study the effects of this traffic-energy imbalance in green networks and to formulate network operation strategies. We present an analytical framework for computing the operator's revenue while fulfilling the users' service guarantee. The revenue maximization problem is solved algorithmically through proposed network operation and green energy allocation strategies. The network is subjected to heterogeneous skewed traffic of varying degrees and operated using two distinct strategies, the conventional without coverage adjustment (WCA) and the proposed cooperative coverage adjustment (CCA) model. In the conventional WCA model the cells do not dynamically adjust their coverage areas, whereas the proposed CCA model involves the radio network controller (RNC) for adjusting the cell coverage areas based on traffic load and energy availability. Our analysis and simulation results demonstrate that the proposed CCA model is highly effective in addressing traffic-energy imbalance at the cellular level and significantly improves the revenue as compared to the conventional WCA model. Our results demonstrate that with the proposed CCA model, the revenue gain increases with an increase in traffic skewness. For example, it provides a gain up to 61% under high (80%) traffic skewness while serving about 25% of more users.

Index Terms—Dual powered cellular network, green communication, resource allocation, revenue maximization, traffic energy balancing

I. Introduction

THE advent of the Internet of Things (IoT) has not only paved way for a massive increase in devices in a communication network, but also resulted in stringent quality of service (QoS) demands from them [2]. The cellular networks are equipped with base stations (BSs) to cater to the demands of user equipment connected to them. These BSs require a

considerable amount of fuel to run without energy outages and to further guarantee the QoS requirements of the users associated with them. The study in [3] estimated that a typical stand-alone BS, i.e., the one not connected to the power-grid, consumes about 1500 liters of diesel per month. It is also estimated that the information and communication technology sector causes about 2% of worldwide carbon emissions, of which about 60% come from the BSs [4].

Thus, the ever-standing problem of traffic load management [5] along with minimizing BS power consumption envisioning green communication, faces a major challenge in the upcoming years of the IoT-enabled 5G communications [6]. Using renewable energy sources like solar energy [7] is being considered as a possible solution to minimize the carbon footprint generated by BSs. While purely solar-enabled BSs are effective in reducing the carbon footprint, they are not economically viable to the operators [8] and are prone to energy outages. Hence, solar-enabled and power-grid connected 'dual-powered' cellular networks have become attractive. Designing a dual-powered network is challenging due to the stochastic nature of solar harvest and spatio-temporal variation of user traffic. This may lead to a traffic-energy imbalance, where some BSs may have more traffic than they can handle, and some BSs may not have sufficient number of users to serve their capacity. A formal definition of traffic-energy imbalance is provided below.

Definition 1. *Traffic-energy imbalance is defined as a scenario in dual-powered cellular networks, wherein due to spatio-temporal variation of user density and stochastic nature of harvested energy, a BS is either unable to serve all the users in its coverage range with its energy reserve or it has surplus energy compared to that required to serve the current traffic.*

A dual-powered network operation involves various cost metrics accounting for the various costs incurred by an operator and sources of revenue generation. These metrics include the cost of installing the network, called capital expenditure (CAPEX) [8], cost incurred to avert energy outages, called operational expenditure (OPEX) [9], revenue earned by selling excess energy back to the grid, and the revenue earned by serving users in the network.

Thus, one of the main motivations of this study is to observe the effect of traffic-energy imbalances on the revenue of a cellular network operator. We devise novel network operation strategies to maximize revenue while guaranteeing user service requirements. Another motivation behind this study is to observe this traffic-energy imbalance in the presence of heterogeneous traffic. This is investigated by devising a novel

queuing model based cross-layer analysis for differentiating the traffic as either delay-constrained or delay-tolerant at the BS depending on certain 3GPP defined QoS parameters. In the upcoming sub-section we will discuss the related works following the contributions and paper layout.

A. State-of-the-art

So far, the research conducted to cater to the vision of green communication have relied on energy saving strategies like optimum resource allocation [5], [10], [11], intelligent BS switching techniques [12], [13], and cell-zooming techniques [14]. The strategies such as dynamic BS ON/OFF or cell breathing techniques are also called traffic management techniques. The authors in [15] presented a comprehensive survey on the modeling and analysis of energy harvesting in grid-powered wireless networks. Optimal resource allocation strategies [5], [10] studied general cellular networks, providing a tractable framework for flexible user association, maximizing the cell capacity, and spectral efficiency. The analysis in [11] presents a comprehensive study on designing cross-layer communication systems with energy constraints. Intelligently switching the BSs depending on the traffic load [12], [13] and cell zooming techniques [14] were also useful in reducing the network power consumption. The study in [16] presented an efficient MDP based user association strategy in super-WiFi networks, representing a BS state jointly based on the number of users associated and the battery level.

Dual-powered networks also face challenge in dealing with stochastic environments [17]. The randomness in traffic, harvested energy, and channel conditions need to be considered to make the problem more practical. The works presented in [8], [18], and [19] considered the randomness of traffic and harvested energy but did not consider randomness in channel variations. The framework presented in [19] dealt with designing purely solar powered off-grid systems. Even though it considered random traffic, the traffic nature was homogeneous. The user traffic generated for the users associated with the BS can be heterogeneous in nature. The study in [20] dealt with minimizing the grid consumption of mixed traffic green networks, where user satisfaction for each traffic class was represented using utility functions [21].

Traffic-energy imbalance has been presented in recent studies [22], [23], [24], and [25]. The analysis in [22] studies cellular networks subjected to spatial distributions of traffic load and power consumption, without dealing with green energy or dual-power supplies. The framework in [23] presents an energy-efficient traffic offloading approach in heterogeneous networks. The framework in [24] analyzes spatial modeling of traffic in cellular networks, while the study in [25] presents a framework for a traffic-aware BS sleeping control strategy to reduce power consumption. While the traffic generated in [24] and [25] are stochastic, they do not consider spatio-temporal traffic variations across the network. In our recent preliminary study [1], we have analyzed traffic skewness aware green networks with a given solar dimensioning and addressed the traffic-energy imbalance due to spatio-temporal traffic variations at the cellular level.

In [1], we have solved the skewed traffic dependent energy imbalance at the BSs through a novel energy balancing scheme wherein the cell coverage areas were adjusted by the radio network controller (RNC) as a function of user density and BSs energy availability. In this work, we continue to develop this idea by incorporating a cross-layer analysis combining the network, medium access control (MAC), and physical layer aspects, and subject the users associated with BS to heterogeneous skewed traffic. We provide a tractable form for the minimum rate required by a user service irrespective of whether the arriving traffic is delay-constrained or delay-tolerant, a lower bound for the minimum power that can be allotted on a subcarrier, and showcase some network operating strategies along with the associated operator revenues.

B. Contributions

Key features and contributions of this work are as follows:

1) We present an analytical framework to capture the effects of traffic-energy imbalance on the revenue of network operator and propose a cooperative cellular coverage adjustment based traffic-energy imbalance mitigation strategy in a dual-powered cellular network with a given solar dimensioning.

2) The revenue earned by a network operator is mathematically modeled and is observed to be an NP-hard problem. The optimization problem is algorithmically solved for network operation and green energy allocation. The network subjected to traffic of varying skewness levels is operated with two distinct strategies: the conventional without coverage adjustment (WCA) model and the proposed cooperative coverage adjustment (CCA) model. These strategies are compared in terms of average users served and the revenue gain. Also a tradeoff between complexity of the proposed CCA model and the operator revenue as a function of coverage adjustment frequency is investigated.

3) The traffic subjected to the network is considered to be heterogeneous. A tractable lower bound of the rate required for a user is derived as a function of QoS parameters defined by 3GPP [26] and the expected rate of arrival of packets, irrespective of the traffic class.

4) After computing the user QoS, the optimal resource allocation comprising of subcarrier and power assignment is performed. A lower bound for the minimum power required per subcarrier assigned to a user is derived depending on the rate required by the user, as per the queue and channel information. Further, the BS downlink transmit power is calculated.

5) The simulation results demonstrate an increasingly higher impact of the proposed coverage adjustment based model in terms of number of users served and revenue gain, with the increase of traffic-energy imbalance. For example, the proposed coverage adjustment model serves 0.05% more users with a net revenue gain of 0.006% at 17% traffic imbalance, whereas it serves about 25% more users with a net revenue gain of about 61% at 80% traffic imbalance. This demonstrates the significance of addressing traffic-energy imbalance in a dual-powered cellular network

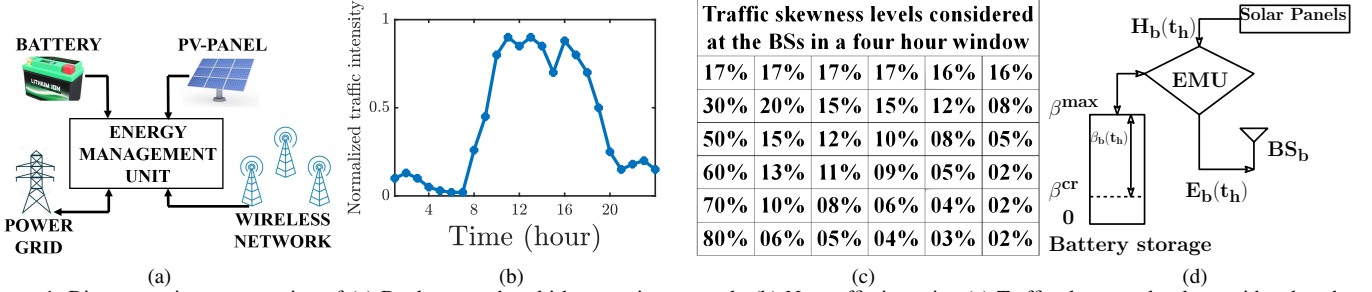| Traffic skewness levels considered at the BSs in a four hour window					
17%	17%	17%	17%	16%	16%
30%	20%	15%	15%	12%	08%
50%	15%	12%	10%	08%	05%
60%	13%	11%	09%	05%	02%
70%	10%	08%	06%	04%	02%
80%	06%	05%	04%	03%	02%

Figure 1: Diagrammatic representation of (a) Dual powered multi base station network, (b) Net traffic intensity, (c) Traffic skewness levels considered at the BSs in a time window (d) Energy dynamics in a solar-enabled BS.

C. Organization

The organization of this paper is as follows. Section II introduces the system model and the problem objective briefly. In Section III, we compute the user QoS requirements in presence of heterogeneous traffic, perform the resource allocation and calculate the average achievable user rate. Section IV presents the NP-hard operator revenue maximization formulation along with the algorithms developed to solve the NP-hard problem. In Section V, presents the system performance results. Section VI concludes the paper.

II. SYSTEM MODEL AND OBJECTIVE

We consider the downlink of a dual powered, multi-BS wireless communication network subjected to skewed traffic. A solar-enabled and power-grid connected BS network is illustrated in Fig. 1(a). We consider a set of B BSs, represented as $\mathbf{B} = \{1, 2, \cdots, B\}$, and a set $\mathbf{U}$ comprising of $\mathcal{U}$ active users following a Poisson point process (PPP) having average user density λ_u in a fixed area A. It is assumed that the users cannot move out of the area under observation but can displace within. We also assume that each user is being served by only one BS, although the user may fall in the coverage area of more than one BS at a time instant.

The user locations are used to compute the optimum BS locations and coverage areas using K-means clustering algorithm. At the initial design and deployment stage, the users are assumed to associate with the BSs following maximum received power level criterion, with the downlink transmit power of the BSs being assumed equal and denoted as $\mathbf{P} = \{P_b\} \ \forall \ b \in B$, such that $0 \leq P_b \leq P_{max}$ with P_{max} being the peak downlink transmit power constraint. Thus the total number of users associated with each BS b is given by $\mathbf{U} = \{N_1, \cdots, N_B\} \ \forall \ b \in B$, such that $\mathcal{U} = \sum_{b=1}^{B} N_b$. The coverage radius of the base stations at this initial stage is represented by $\mathbf{R} = \{R_1, R_2, \cdots, R_B\}$. Further, the total system bandwidth available is denoted as BW with the BSs assumed to operate in full frequency reuse mode. The set $\mathbf{S}$ of subcarriers is given as $\mathbf{S} = \{1, 2, \cdots, S_m\}$, with the resulting frequency spacing between the subcarriers being $\Delta f = BW/S_m$. The traffic profile is discussed in the following subsection.

A. Traffic profile

We consider that the BSs are subjected to skewed traffic. The net traffic profile $\rho(t_h)$ over the entire area A is shown in Fig. 1(b), which has been generated as per the data collected in [27]. The packets are assumed to follow Poisson process of hourly varying average intensity given in Fig. 1(b). We consider that the traffic subjected to a BS b, $\rho_b(t_h) = N_b(t_h)/\sum_{b=1}^{B} N_b(t_h)$, is highly skewed at any hour t_h of the day. From the purpose of analyzing the possible traffic-energy imbalance in the network, we divide the full day into six windows of four hours each. A formal definition of traffic skewness level as used throughout this paper is given below.

Definition 2. *Traffic skewness is defined as the maximum fraction of network traffic intensity subjected to a BS.*

A BS is subjected to skewed traffic within a time window, such that some other BS experiences skewed traffic as the day progress, as portrayed through Figs. 2(a) - 2(f). For example, Fig. 2(f) represents 80% traffic skewness such that, at any hour, a BS coverage area has 80% of the net traffic in Fig. 1(b). The remaining BSs are subjected to the fraction of traffic intensities shown in the last row of Fig. 1(c). For result generation purposes, we have considered area A to be covered by six BS. The various traffic skewness levels considered in one window at the BSs are shown in Fig. 1(c). Our analysis includes all possible permutations having these traffic skewness levels.

The user traffic arrivals are assumed to belong to two specific traffic classes, delay-constrained (DC) $\rho_{DC}(t_h)$ and delay-tolerant (DT) $\rho_{DT}(t_h)$, such that $\rho_b(t_h) = \rho_{DC}(t_h) + \rho_{DT}(t_h)$. We assume that at any BS b at hour t_h, the average arrival rate of the delay-constrained and delay-tolerant traffic is $\eta\%$ and $(100 - \eta)\%$ respectively, of the net average traffic subjected on the BS b. We briefly describe objective of this work before delving into greater details in coming sub-section.

B. Objective

We aim to design revenue aware network operation strategies such that the traffic-energy imbalance generated due to spatio-temporal variations can be addressed in the network. Before detailing the cost metrics involved in a network operation, we briefly discuss the energy dynamics of a green BS as illustrated in Fig. 1(d). It shows the various energies involved in a solar-enabled green BS. Each BS is equipped with a battery storage having N_{Batt} number of batteries, having a capacity β^{cap} each and N_S solar panels. The maximum energy storage capacity with each BS will thus be $\beta^{max} = N_{Batt}\beta^{cap}$, with the critical level below which energy can not be extracted

(a) 17% traffic skewness (average)

(b) 30% traffic skewness (moderate)

(c) 50% traffic skewness

(d) 60% traffic skewness
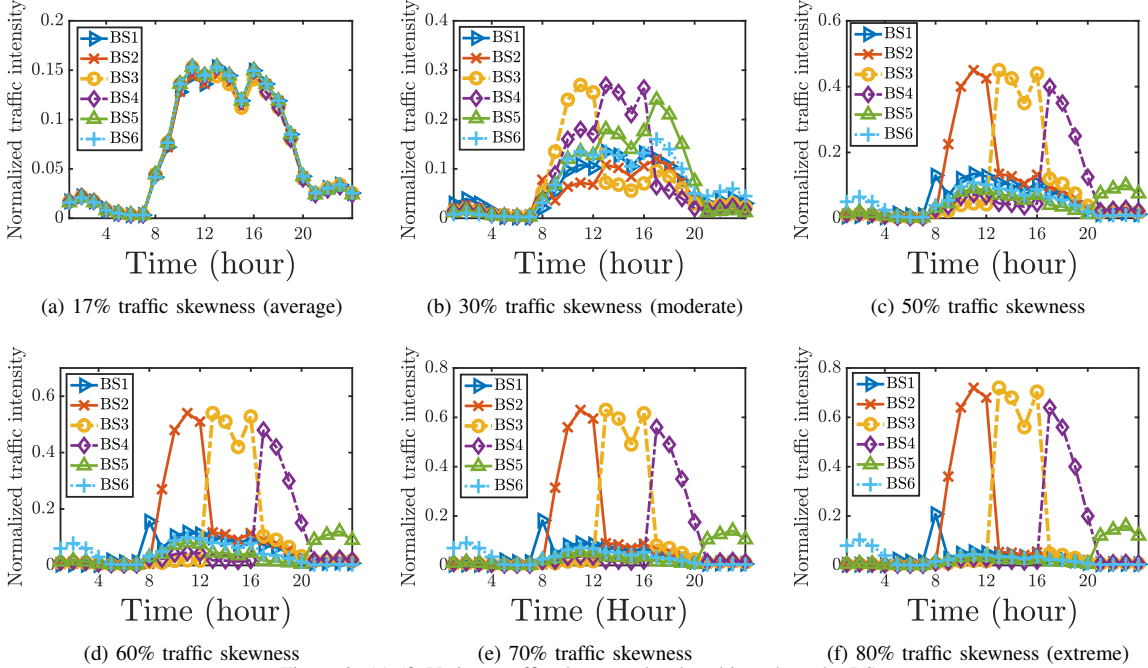
(e) 70% traffic skewness

(f) 80% traffic skewness (extreme)

Figure 2: (a)-(f) Various traffic skewness levels subjected on the BSs.

represented as $\beta^{cr} = \delta N_{Batt} \beta^{cap}$. Here δ is the depth of discharge decided by the operator to avoid battery degradation. Energy can be either extracted from the battery as required by the BS load or simultaneously stored in it as harvested by the PV panels.

We have obtained the hourly energy harvested by a 1KW rated PV panel as shown in Fig. 1(d), using the annual solar radiation data provided by National Renewable Energy Laboratory, which is fed into System Advisor Model [28]. Let the hourly net energy harvested for a BS enabled with N_S unit rated panels be $H_b(t_h)$. We denote the hourly net energy consumption by a BS b as $E_b(t_h) = (P_0 + P_b(t_h))$, with P_0 denoting the static power consumption in addition to the dynamic consumption $P_b(t_h)$ due to hourly varying traffic. With the discussed energy dynamics in a dual-powered BS, the hourly battery level $\beta_b(t_h)$ is computed as follows:

$$\text{Let } \beta'_b(t_h) = \beta_b(t_h - 1) + H_b(t_h) - E_b(t_h).$$
$$\text{Then, } \beta_b(t_h) = \min\left\{\max\left\{\beta'_b(t_h), \beta^{cr}\right\}, \beta^{max}\right\}. \quad (1)$$

It is notable that in an energy-deficient BS b, i.e., if $\beta'_b(t_h) \leq \beta^{cr}$, the hourly deficient energy to be purchased from the power grid is $E_b^d(t_h) := |\beta'_b(t_h) - \beta^{cr}|$. Likewise, in an energy-surplus BS b, i.e., if $\beta'_b(t_h) \geq \beta^{max}$, the hourly surplus energy of the BS to be sold back to the power grid is $E_b^S(t_h) := (\beta'_b(t_h) - \beta^{max})$.

We now classify the costs related to a network operation strategy into four metrics, with the first metric called CAPEX, referring to the investments to be borne by the operator related to dimensioning the BSs. The second metric called OPEX, refers to the cost incurred by the operator when a BS b becomes energy-deficient and is calculated as $\text{OPEX} = \sum_{b=1}^{B} \sum_{t_h=1}^{24} \left(c_{buy} E_b^d(t_h)\right)$. The energy-surplus scenario involves a third cost metric, called revenue by

selling surplus energy R_{sell} which is calculated as $R_{sell} = \sum_{b=1}^{B} \sum_{t_h=1}^{24} \left(c_{sell} E_b^S(t_h)\right)$. Here c_{sell} and c_{buy} are the respective costs to sell and buy unit energy, to and from the power-grid. The operator earns revenue by fulfilling the QoS requirements of the users $\mathcal{U} = \sum_{b=1}^{B} N_b$ in the network. This fourth revenue metric is termed as revenue by serving R_{serv}, which can be computed as $R_{serv} = \sum_{b=1}^{B} \sum_{t_h=1}^{24} (c_{serv} N_b(t_h))$, with c_{serv} being the daily revenue earned by serving a user. Here, $N_b(t_h)$ refers to hourly number of users whose QoS is being met by BS b. These cost metrics will be presented in detail in Section IV. Thus, a general unconstrained optimization problem can be written as

$$\max \text{ Revenue} = \max\left(R_{serv} + R_{sell} - \text{OPEX} - \text{CAPEX}\right). \quad (2)$$

In this paper, we look to compute the hourly optimum values of $N_b(t_h) \, \forall \, b \in B$, hourly deficient energy required $E_b^d(t_h) \, \forall \, b \in B$, and the hourly surplus energy $E_b^S(t_h) \, \forall \, b \in B$ possessed with the BSs in the network using the network operation and green energy allocation strategies detailed in Section IV. This in turn aids in computation of the net revenue earned by the operator and solve the revenue maximization problem formulation presented in Section IV. Through this paper, we propose and analyze a cooperative coverage adjustment approach to mitigate the effects of traffic-energy imbalance to enhance the operator revenue. We also study the effects of coverage overhead variation on the operator revenue.

The following section describes the computation of user QoS requirements, the packet scheduling strategy deployed

Table I: 3GPP defined QoS requirements

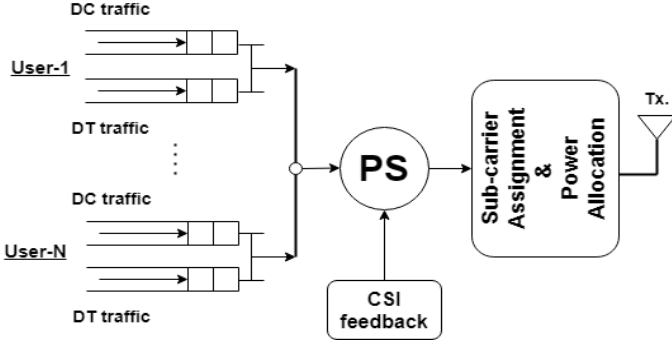| Resource type	τ	P^{pler}	Example services
Delay constrained	100ms	10^{-2}	voice or live streaming
Delay tolerant	300ms	10^{-6}	TCP/FTP based services

Figure 3: Packet scheduler representation.

at the BS to serve the arriving packets, and the resource allocation.

III. RESOURCE ALLOCATION AND ACHIEVABLE RATE CALCULATION

A block diagram of the packet scheduler (PS) implemented at each BS b is shown in Fig. 3. The PS at BS b receives along with the packets generated by the active users associated with that BS, the channel state information (CSI) of each user at the various sub-carriers as input. We assume perfect CSI feedback from the users and that the channel state remains static over a time slot. Since the users can generate traffic belonging to either of the traffic classes with average arrival rates λ_{DC} or λ_{DT} respectively, for delay-constrained and delay-tolerant traffic. It is considered that each user $u \in N_b$ associated with BS b, has its separate and independent set of queues for each traffic class [29]. This assumption has been considered for the adherence to QoS of users belonging to different service classes. The following sub-section presents a queuing analysis for computing the user QoS requirements.

A. Proposed QoS aware queuing model

Let each packet generated by a user $u \in N_b$ have a QoS requirement given by $\{P^{pler}, \tau\}$, representing the packet loss error rate (PLER) and target packet delay, respectively. These QoS metrics vary according to the traffic class of packet as per the 3GPP LTE specifications as listed in Table I. It is notable from Table I that delay-constrained traffic packets have a very stringent delay budget but can afford a higher packet loss rate. On the other hand, packets that are delay-tolerant have a very tight PLER budget. We begin the classical queuing analysis by deriving the rate required by each user as a function of the QoS parameters and the average rate of packet arrival. We consider the buffer queue length of each user $u \in N_b$ as B_Q for both traffic classes. Let $L_u(t)$ denote queue length of buffer for user u at time slot t. Then the queue length of user u at the next time slot $(t + 1)$ is found as

$$L_u^+(t+1) = \max\{\left(L_u(t) - \overline{r_{ub}(t_h)}T_f/N_{bits} + a_u(t)\right), 0\}. \quad (3)$$

Considering the buffer limit B_Q, the updated queue length in time slot $(t + 1)$ would be

$$L_u(t + 1) = \min\{B_Q, L_u^+(t + 1)\} \quad (4)$$

where $\overline{r_{ub}(t_h)}$ denotes the average rate achievable for user u when associated with BS b at hour t_h, T_f denotes the number

of frames which are served simultaneously, and N_{bits} represent the number of bits per packet. Packet size is considered fixed for both traffic classes. It can be observed that the term $\overline{r_{ub}(t_h)}T_f/N_{bits}$ in (3) denotes the number of queued packets of user u which are served at time slot t. Further $a_u(t)$ denotes the number of packets generated by user u, and its value depends on the traffic class of the packet, given by

$$\mathbb{E}\{a_u(t_h)\} = \begin{cases} \lambda_{DC}, & \text{if arriving packets are delay-constrained} \\ \lambda_{DT}, & \text{if arriving packets are delay-tolerant.} \end{cases} \quad (5)$$

The number of packets for user u getting dropped at the end of time slot t is given by

$$D_u(t + 1) = \max\{0, L_u(t + 1) - B_Q\} + \nu(t) \quad (6)$$

where, the first term represents packet drop due to buffer overflow and $\nu(t)$ represents the number of packets getting dropped due to packet delay violation at the end of slot t.

We compute the average delay incurred by a user u at the end of time-slot t based on Little's theorem [30], which is expressed as

$$\tau_u(t + 1) = \frac{\overline{L_u(t + 1)}}{\mathbb{E}\{a_u(t_h)\}} \leq \tau. \quad (7)$$

where $\overline{L_u(t + 1)}$ denotes the average queue length at the beginning of $(t + 1)^{th}$ slot. It is given as equation (8) below with t_w being the window in which averaging is performed.

$$\overline{L_u(t+1)} = \left(1 - \frac{1}{t_w}\right)\overline{L_u(t)} + \frac{L_u(t + 1)}{t_w}$$
$$= \left(1 - \frac{1}{t_w}\right)\overline{L_u(t)} + \left(\frac{L_u(t) - \frac{\overline{r_{ub}(t_h)}T_f}{N_{bits}} + a_u(t)}{t_w}\right). \quad (8)$$

It is notable that, we use Little's theorem for mathematically capturing the packet delay, as it is applicable only for average statistics, such as average arrival rate and average queue length. Hence, we compute the average delay experienced by a user in a time slot (over a small window t_w) and further decide on the delay violation of packets. Since we aim to develop an analytical framework for heterogeneous traffic that can distinguish the services as delay-tolerant or delay-constrained, an upper bound on this delay computed is required. In absence of any standard specification on average delay limit, as a loose constraint, we compare the average delay incurred with the standard 3GPP defined delay budget. System performance with this approximation is evaluated in Section V-B. Using (7) and (8), the delay budget constraint to be guaranteed by the PS can be expressed as

$$\tau \geq \frac{\left(1 - \frac{1}{t_w}\right)\overline{L_u(t)} + \left(\frac{L_u(t) - \frac{\overline{r_{ub}(t_h)}T_f}{N_{bits}} + a_u(t)}{t_w}\right)}{\mathbb{E}\{a_u(t_h)\}}$$

which reduces to,

$$\overline{r_{ub}(t_h)} \geq \frac{N_{bits}}{T_f}\left((t_w - 1)\overline{L_u(t)} + L_u(t) + a_u(t) - \mathbb{E}\{a_u(t_h)\}\tau t_w\right). \quad (9)$$

Therefore, we infer that the achievable rate of user u is a

function of the QoS parameter, i.e., the delay budget. Further, to satisfy the packet loss rate constraint for a user, the PS needs to ensure the following condition:

$$P_u^{pler}(t+1) = \frac{\overline{D_u(t+1)}}{\mathbb{E}\{a_u(t_h)\}} \le P^{pler} \qquad (10)$$

where $\overline{D_u(t+1)}$ denotes the average number of packets dropped at the end of time slot t. This can be further expressed as

$$P^{pler} \ge \frac{\max\{\overline{L_u(t+1)} - B_Q, 0\} + \nu(t)}{\mathbb{E}\{a_u(t_h)\}}. \qquad (11)$$

Solving for the case of nonzero packet drop due to buffer overflow, it follows that

$$P^{pler} \ge \frac{\overline{L_u(t+1)} - B_Q + \nu(t)}{\mathbb{E}\{a_u(t_h)\}}$$

or, $P^{pler}\mathbb{E}\{a_u(t_h)\} \ge \left(1 - \frac{1}{t_w}\right)\overline{L_u(t)} + \frac{L_u(t+1)}{t_w} - B_Q + \nu(t)$

which reduces to,

$$\frac{\overline{r_{ub}(t_h)}T_f}{N_{bits}} \ge (t_w - 1)\overline{L_u(t)} + L_u(t) + a_u(t)$$
$$- B_Q + \nu(t) - P^{pler}\mathbb{E}\{a_u(t_h)\}t_w.$$

Finally we obtain

$$\overline{r_{ub}(t_h)} \ge \frac{N_{bits}}{T_f}\left((t_w - 1)\overline{L_u(t)} + L_u(t) + a_u(t) \right.$$
$$\left. - B_Q + \nu(t) - P^{pler}\mathbb{E}\{a_u(t_h)\}t_w\right). \qquad (12)$$

Therefore, we again observe that the rate achievable by user u is a function of the second QoS parameter, i.e., the packet loss rate. We denote certain right hand side terms of (9) as $\kappa = \left((t_w - 1)\overline{L_u(t)} + L_u(t) + a_u(t)\right)$ and certain right hand side terms of (12) as $\kappa' = \left((t_w - 1)\overline{L_u(t)} + L_u(t) + a_u(t) - B_Q + \nu(t)\right)$. Finally combining (9) and (12), we have

$$\overline{r_{ub}(t_h)} \ge \frac{N_{bits}}{T_f}\max\left\{(\kappa - \tau\mathbb{E}\{a_u(t_h)\}t_w), \left(\kappa' - P^{pler}\mathbb{E}\{a_u(t_h)\}t_w\right)\right\}$$
$$= f\left(\tau, P^{pler}\right). \qquad (13)$$

The expression (13) represents a general, tractable lower bound for the rate required by user u associated with BS b as a function of the QoS parameters.

The following sub-section deals with the subcarrier assignment and calculation of $\overline{r_{ub}(t_h)}$ in accordance with physical layer parameters.

B. Subcarrier assignment and achievable average rate calculation

After computing the user QoS requirement, depending on the number of packet arrival for each user and the CSI feedback, the PS assigns a subcarrier set to each user. Orthogonal frequency division multiplexing (OFDM) based physical layer resource allocation [31] is performed to allot time-frequency resource blocks to the users in accordance with their QoS requirements. It is assumed that subcarrier s is not shared with any other users in a given time slot and that each user

---

Algorithm 1: Subcarrier assignment

Result: $\pi_{usb}(t)$

1 **Input:**
   $u \in N_b, \mathbf{S} = \{1, 2, \cdots, S_m\}, BW, d_{ub}, h_{usb}, \sigma^2, P_{max}, L_u(t)$
2 **Initialize:** $P_{usb} = P_{max}/S_m$
3 $r_{usb}(t) = \Delta f \log_2(1 + \text{SINR}_{usb}(t))$.
4 **if** $L_u(t) > 0$ **then**
5      $s \Longleftarrow u,$ if $r_{usb} > r_{u'sb} \ \forall\ u' \in N_b,$ and $u' \ne u$
6   **if** $s \Longleftarrow u$ **then**
7          $\pi_{usb} = 1$
8   **end**
9   **else**
10          $\pi_{usb} = 0$
11   **end**
12 **end**
13 **else**
14   User is removed from service for that time slot
15 **end**

---

gets a distinct subcarrier set at each time slot depending on the subcarrier assignment strategy. Since a resource block is a time-frequency component, we assume a resource block to consist of one transmission time interval (TTI) time unit and one subcarrier frequency component.

Let the user $u \in N_b$ be associated with BS b, located at a distance d_{ub} from it. Let the Rayleigh distributed CSI of the user u associated with BS b at subcarrier s be h_{usb}, having an exponentially distributed channel gain $|h_{usb}|^2 = g_{usb}$ with unit mean. Therefore, with full frequency reuse of bandwidth at each BS b, the signal to interference and noise ratio (SINR) for a user u associated with BS b over subcarrier s at a distance d_{ub} from the BS can be expressed as

$$\text{SINR}_{usb}(t) = \frac{P_{usb}(t)g_{usb}}{d_{ub}^2\sigma^2 + \sum_{b' \in B} P_{u'sb'}(t)g_{u'sb'}d_{u'b'}^{-2}} \qquad (14)$$

where $P_{usb}(t)$ is the power allocated by the BS b to user u over subcarrier s, σ^2 is the variance of additive white Gaussian noise (AWGN) assumed same at all subcarriers, and $b' \in \mathcal{B} - \{b\}$. Depending on the $\text{SINR}_{usb}(t)$, the rate that can be achieved by the user u when associated with BS b on subcarrier s at time slot t is expressed as $r_{usb}(t) = \Delta f \log_2(1 + \text{SINR}_{usb}(t))$.

Algorithm 1 presents the steps used for subcarrier assignment for a user u associated with BS b with downlink transmit power level $\mathbf{P} = \{P_b\} \ \forall\ b \in B$, such that $0 \le P_b \le P_{max}$. In Step 3 we compute the data rate achievable by each user on each subcarrier at each time slot. If the user achieving maximum data-rate does not have an empty queue to serve (Step 4), it is assigned to the user u in Step 5. If user u is allotted subcarrier s, then we assign it an indicator variable $\pi_{usb}(t)$ as 1, else its assigned 0, i.e.,

$$\pi_{usb}(t) = \begin{cases} 1, & \text{if user } u \text{ is alloted subcarrier} s \text{ in time slot } t. \\ 0, & \text{otherwise.} \end{cases} \qquad (15)$$

For computing the average rate achievable by a user over its assigned subcarriers, the distribution of subcarrier rate needs to be ascertained. Since the channel gains $g_{usb}(t)$ are exponentially distributed with unit mean corresponding to the respective Rayleigh distributed channels, the distribution of rate achievable on a single subcarrier is a logarithmic trans-

formation of the exponential random variable. The calculation can be shown as follows: Let

$$Y := r_{usb}(t) = \Delta f \log_2 \left(1 + \frac{P_{usb}(t)g_{usb}(t)}{d_{ub}^2 \sigma^2 + \sum_{b' \in B} P_{u'sb'}(t)g_{u'sb'}d_{u'b'}^{-2}} \right). \tag{16}$$

Taking $\Upsilon = P_{usb}(t)/\left(d_{ub}^2\sigma^2 + \sum_{b' \in B} P_{u'sb'}(t)g_{u'sb'}d_{u'b'}^{-2}\right)$, then $Y(\Upsilon) = \frac{\Delta f}{\ln 2} \ln(1 + \Upsilon g_{usb})$. Thus, the cumulative distribution function (CDF) of Y is

$$F_Y(y) = \mathbb{P}\{Y \le y\} = \mathbb{P}\left\{ \frac{\Delta f}{\ln 2} \ln(1 + \Upsilon g_{usb}) \le y \right\}$$
$$= \mathbb{P}\left\{ g_{usb} \le \frac{e^{Y \ln 2/\Delta f} - 1}{\Upsilon} \right\}. \tag{17}$$

Hence, the probability density function (PDF) of Y is obtained as

$$f_Y(y) = \exp\left(\frac{1 - e^{y \ln 2/\Delta f}}{\Upsilon} \right) \left(\frac{\ln 2}{\Upsilon \Delta f} e^{y \ln 2/\Delta f} \right). \tag{18}$$

The expression (18) is the distribution of rate achievable on a Rayleigh distributed subcarrier for a given $\text{SINR}_{usb}(t)$, Υ. Thus, the mean rate achievable on a subcarrier for a given Υ can be calculated as

$$\overline{r_{usb}(t)} = \int_0^\infty r_{usb}(\Upsilon)f_Y(r)dr = \frac{-\Delta f}{\ln 2} \exp\left(\frac{1}{\Upsilon} \right) \text{Ei}\left(\frac{-1}{\Upsilon} \right) \tag{19}$$

where $\text{Ei}(\cdot)$ is the exponential integral function obtained from [32]. The corresponding average achievable net rate to user u over the subcarriers assigned to it at time slot t is

$$\overline{r_{ub}(t)} = \sum_{s=1}^S \pi_{usb}(t)\overline{r_{usb}(t)}. \tag{20}$$

Further, the time average of rates achievable for a user u at an hour t_h is obtained as

$$\overline{r_{ub}(t_h)} = \frac{\sum_{t=0}^T \left(\sum_{s=1}^S \pi_{usb}(t) \int_0^\infty r_{usb}(\Upsilon)f_Y(r)dr \right)}{T} \tag{21}$$

where T is the total number of time slots considered over an hour duration. The expression (21) gives the average rate achievable by a user over its assigned subcarriers. Next, we discuss the optimum power allocation on each user's assigned subcarrier and the computation of BS downlink transmit level in the following sub-section.

C. Optimum power allocation

Expression (13) obtained from the queuing analysis in Section III-A represents the rate required by a user u when associated with BS b to meet its QoS guarantee. Equating the physical layer rate with (13) in a particular time slot, we get

$$\sum_{s=1}^S \pi_{usb}\Delta f \log_2 \left(1 + \frac{P_{usb}(t)g_{usb}}{d_{ub}^2 \sigma^2 + \sum_{b' \in B} P_{u'sb'}(t)g_{u'sb'}d_{u'b'}^{-2}} \right)$$
$$\ge \frac{N_{bits}}{T_f} \max \left\{ (\kappa - \mathbb{E}\{a_u(t_h)\}\tau t_w), \ \left(\kappa' - P^{pler}\mathbb{E}\{a_u(t_h)\}t_w \right) \right\}. \tag{22}$$

To calculate the optimum power required by a single subcarrier at a given time slot t, we use the fact that the physical layer rate achievable on a single subcarrier should be at most equal to the rate required to meet the QoS requirements, i.e.,

$$\Delta f \log_2 \left(1 + \frac{P_{usb}(t)g_{usb}}{d_{ub}^2 \sigma^2 + \sum_{b' \in B} P_{u'sb'}(t)g_{u'sb'}d_{u'b'}^{-2}} \right)$$
$$\le \frac{N_{bits}}{T_f} \max \left\{ (\kappa - \mathbb{E}\{a_u(t_h)\}\tau t_w), \ \left(\kappa' - P^{pler}\mathbb{E}\{a_u(t_h)\}t_w \right) \right\}. \tag{23}$$

Hence we have

$$\mathbb{P}\left(\Delta f \log_2 \left(1 + \frac{P_{usb}(t)g_{usb}}{d_{ub}^2 \sigma^2 + \sum_{b' \in B} P_{u'sb'}(t)g_{u'sb'}d_{u'b'}^{-2}} \right) \le \overline{r_{ub}(t_h)} \right) \ge p_0$$

$$\text{or, } \mathbb{P}\left(g_{usb} \le \frac{\left(2^{\frac{\overline{r_{ub}(t_h)}}{\Delta f}} - 1 \right)\left(d_{ub}^2 \sigma^2 + \sum_{b' \in B} P_{u'sb'}(t)g_{u'sb'}d_{u'b'}^{-2} \right)}{P_{usb}} \right) \ge p_0. \tag{24}$$

where p_0 is the probability associated with channel inversion used. Since the channel gains are exponentially distributed with unit mean, the equation (24) can be further solved as

$$1 - \exp\left(-\frac{\left(2^{\frac{\overline{r_{ub}(t_h)}}{\Delta f}} - 1 \right)\left(d_{ub}^2 \sigma^2 + \sum_{b' \in B} P_{u'sb'}(t)g_{u'sb'}d_{u'b'}^{-2} \right)}{P_{usb}} \right) \ge p_0.$$

Thus it follows that,

$$P_{usb}(t) \ge \frac{\left(1 - 2^{\frac{\overline{r_{ub}(t_h)}}{\Delta f}} \right)\left(d_{ub}^2 \sigma^2 + \sum_{b' \in B} P_{u'sb'}(t)g_{u'sb'}d_{u'b'}^{-2} \right)}{\ln(1 - p_0)}. \tag{25}$$

Expression (25) represents a lower bound for the minimum power which has to be allocated to a subcarrier s for user u when associated with BS b to meet its QoS guarantee. Further, the net power allocated to a user over all the subcarriers allotted to it is given as, $P_{ub}(t) = \sum_{s=1}^S \pi_{usb}(t)P_{usb}(t)$. Therefore, the net downlink power level required to be allocated to all the users for satisfying their individual QoS requirements in time slot t is given as

$$P_b(t) = \sum_{u=1}^{N_b(t_h)} P_{ub}(t) \le P_{max}. \tag{26}$$

Finally, the average downlink transmit power level over an hour will be then calculated as

$$P_b(t_h) = \frac{\sum_{t=1}^T P_b(t)}{T} \le P_{max}. \tag{27}$$

It can be noted that (26) ensures that $P_{usb}(t)$ is allocated such that it satisfies the peak-power constraint mandated by the federal communications commission (FCC). Now, that we have defined the user QoS requirement and have performed the resource allocation, we will reformulate the earlier unconstrained optimization problem (2) in the following section.

IV. PROPOSED STRATEGY FOR REVENUE MAXIMIZATION

We aim to maximize the annual revenue earned by the network operator as a function of the number of users associated with the network and the BS downlink transmit power. We

start with a detailed introduction to calculating the cost metrics introduced in Section II-B.

A. Revenue maximization problem formulation

1) *CAPEX:* We define CAPEX as the investments borne by the operator for dimensioning the BSs. Considering the unit cost of PV panels C_S having a life expectancy $\mathcal{L}_S$ and unit cost of storage batteries C_B having a life expectancy $\mathcal{L}_B$, CAPEX is computed as

$$\text{CAPEX} = \frac{C_S N_S}{\mathcal{L}_S} + \frac{C_B B_{Batt}}{\mathcal{L}_B}. \tag{28}$$

Life expectancy of a solar panel is typically constant ($\mathcal{L}_S$ = 25 years [33]), whereas lifetime of storage battery is dependent on the number cycles it operates [8]. $\mathcal{L}_B$ is computed using the framework in [8], which accounts for the number of cycles, operating temperature T_c (in Celsius), and depth of discharge δ.

2) *OPEX:* We define OPEX as the dynamic costs incurred during the BS operations. Since we are doing an annual cost analysis, we assume that no component replacement costs will be incurred. Hence, only the cost of buying unit energy $\left(c_{buy} = \text{USD } 0.079\$\right)$ [34] from the grid to meet the deficient energy requirements is considered to be OPEX, which is further calculated as

$$\text{OPEX} = \sum_{d=1}^{365} \sum_{b=1}^{B} \sum_{t_h=1}^{24} c_{buy} E_b^d(t_h)$$
$$= \sum_{d=1}^{365} \sum_{b=1}^{B} \sum_{t_h=1}^{24} c_{buy}(\beta^{cr} - \beta_b(t_h)). \tag{29}$$

3) R_{sell}: The operator can earn revenue from two main sources: serving users and selling excess energy back to grid. If $\left(c_{sell} = \text{USD } 0.057\$\right)$ [35] be the cost of selling unit energy back to grid, then revenue earned by selling excess energy is computed as

$$R_{sell} = \sum_{d=1}^{365} \sum_{b=1}^{B} \sum_{t_h=1}^{24} c_{sell} E_b^S(t_h)$$
$$= \sum_{d=1}^{365} \sum_{b=1}^{B} \sum_{t_h=1}^{24} c_{sell}(\beta_b(t_h) - \beta^{max}). \tag{30}$$

4) R_{serv}: If c_{serv} = USD 1.31$ [36] is the daily revenue earned by serving a user, then

$$R_{serv} = \sum_{d=1}^{365} \sum_{b=1}^{B} \sum_{t_h=1}^{24} c_{serv} N_b(t_h) \tag{31}$$

is calculated in accordance with the number of users served annually throughout the network.

Finally, the net annual profit or revenue earned by the network operator is calculated as Revenue = R_{serv} + R_{sell} − CAPEX − OPEX.

The unconstrained optimization problem in (2) now becomes a constrained optimization problem due to the derived QoS and power allocation constraints. The reformulated expression for revenue by incorporating the metric definitions and on further solving using (1) for an annual analysis comes to be

$$\text{Revenue} = \sum_{d=1}^{365} \sum_{b=1}^{B} \sum_{t_h=1}^{24} [c_{serv} N_b(t_h) + (c_{sell} + c_{buy})(\beta_b(t_h - 1)$$
$$+ H_b(t_h) - P_0 - P_b(t_h)) - c_{sell}\beta^{max} - c_{buy}\beta^{cr}] - (C_S N_S + C_B N_{Batt}). \tag{32}$$

From (32) we observe that except $N_b(t_h)$ and $P_b(t_h)$, all the other variables are constants at the hour t_h, denoted by $\xi(t_h)$. Constraining (32) by the BS downlink transmit power level constraint (27) and the QoS rate requirement (13), the reformulated constrained revenue maximization problem can be expressed as

$$\max_{N_b(t_h), P_b(t_h)} \sum_{d=1}^{365} \sum_{b=1}^{B} \sum_{t_h=1}^{24} \left[c_{serv} N_b(t_h) - P_b(t_h)(c_{sell} + c_{buy}) + \xi(t_h)\right] - (C_S N_S + C_B N_{Batt}) \tag{33}$$

$$\text{s.t. } 0 \leq P_b(t_h) \leq P_{max} \in \mathbb{R}^+ \tag{34}$$

$$N_b(t_h) \geq 0 \in \mathbb{Z}^+ \tag{35}$$

$$N_b(t_h) := \left\{u : \overline{r_{ub}(t_h)} \geq \frac{N_{bits}}{T_f} \max\left\{\left(\kappa - \mathbb{E}\{a_u(t_h)\}\tau t_w\right), \left(\kappa' - P^{pler}\mathbb{E}\{a_u(t_h)\}t_w\right)\right\}\right\}. \tag{36}$$

Here (36) is not a constraint on the optimization problem, but is rather implicitly defined for completeness to show the fulfillment of the rate guarantee of a user service.

The formulated problem is observed to have two decision variables $N_b(t_h)$ and $P_b(t_h)$ for each BS at each hour. Hence the revenue maximization problem (33) jointly allocates subcarrier and power to the users associated with the BSs and further computes the revenue earned by the operator. The variable $N_b(t_h)$ will always lie in positive integer space $\mathbb{Z}^+$, while $P_b(t_h)$ can lie in the positive real space $\mathbb{R}^+$. Thus the formulated revenue maximization problem being a mixed-integer non-convex programming problem is non-deterministic polynomial time (NP)-hard in nature. As problem (33) is not mathematically tractable further without relaxing the problem and constraints, we have algorithmically obtained solution of the problem. The revenue computation strategy has been decoupled into two parts. The first part involves computation of the hourly user association at each BS $N_b(t_h)$ using the conventional WCA and the proposed CCA model. The second part deals with hourly allocation of energy $P_b(t_h)$ based on the battery levels of each BS using the green energy allocation algorithm.

B. Network operation strategies

In this sub-section we discuss the distinct network operation and green-energy allocation strategies employed.

1) Conventional: Without coverage adjustment (WCA) strategy

As the cellular network is subjected to skewed traffic of varying degrees, the spatio-temporal variation of user traffic results in some BSs getting more user traffic density than others. In such a scenario, the network operator can operate the network with two distinct strategies: the conventional WCA model and the proposed CCA model. The primary objective of the network is to guarantee QoS to the users $u \in N_b(t_h) \forall b \in B$ associated with the respective BSs. The conventional WCA model involves operating a cellular network without having the flexibility to change the cellular radius of the BSs and is presented in Algorithm 2. The BSs which are subjected to skewed traffic at that hour, look to shrink their coverage areas so as to meet the peak power constraint (27) and serve as many users as possible.

The conventional WCA model presented in Algorithm 2 returns, the number of users who are unable to be served $Uns_b(t_h)$ by BS b at hour t_h, the modified BSs coverage radius $R_b^n(t_h)$, the BS transmit power levels $P_b(t_h)$, and the new hourly number of users being served $N_b^n(t_h)$ by BS b as output. The model initially computes the transmit power level at each BS depending on the skewed traffic it is subjected to in Step 5. If the peak power constraint is found to be violated at any BS (Step 6), then the BS decrements its radius by ϵ, which represents the cell coverage decrement parameter. (Step 8). The RNC keeps track of the change of radius $\Delta R_b(t_h)$ in Step 9. The new reduced number of users being served $N_b^n(t_h)$ are computed at each iteration, and the transmit power constraint is checked recursively in Step 14. The worst-case time complexity of the conventional WCA model is observed to be $O(f_{WCA} \times B \times \Lambda)$, where f_{WCA} denotes the iterations performed by the WCA algorithm on a daily basis. The values of Λ depends on the traffic skewness level considered and is reproduced in Table II. Λ denotes the maximum number of iterations required for the algorithm to converge to the peak power constraint.

The conventional WCA algorithm is observed to be poor in addressing the traffic-energy imbalance across the network especially at higher skewed traffic levels, resulting in some BS's being energy-deficient or having surplus energy at different hours throughout the day. This leads to lot of energy with the BSs going unused, which otherwise could have been used to improve the network performance. It is observed that this poor handling of traffic-energy imbalance leads to serving lower number of users on average and a significant loss of revenue, which will be discussed later in Section V. We address this traffic-energy imbalance and improve the network performance using our proposed coverage-based algorithm.

2) Proposed: Cooperative coverage adjustment (CCA) strategy

To cater to the shortcomings of the conventional WCA model, we propose a cooperative coverage adjustment based

---

Algorithm 2: Without coverage adjustment (WCA) based strategy

---

Result: $Uns_b(t_h), P_b(t_h), R_b^n(t_h), N_b^n(t_h)$

1   **Input:** $B, \mathcal{U}, BW, \sigma^2, p_0, R_{des} = R_b(t_h), \rho_b(t_h), P_{max}, \epsilon$

2   **Initialize:** $\rho_b^n(t_h) = \rho_b(t_h), N_b^n(t_h) = N_b(t_h), R_b^n(t_h) = R_b(t_h), Uns_b(t_h) = 0, \Delta R_b(t_h) = 0$

3   **for** $t_h = \{1, 2, \cdots, 24\}$ **do**

4   **for** $b = \{1, 2, \cdots, B\}$ **do**

5   Obtain $P_b(t_h)$ for given $\rho_b(t_h)$ & $R_b(t_h)$

6   **if** $P_b(t_h) \geq P_{max}$ **then**

7   **while** $P_b(t_h) \geq P_{max}$ **do**

8           $R_b^n(t_h) = R_b^n(t_h) - \epsilon$

9           $\Delta R_b(t_h) = R_b(t_h) - R_b^n(t_h)$

10   update $N_b(t_h)$

11           $\rho_b^n(t_h) = N_b(t_h)/\mathcal{U}$

12           $N_b^n(t_h) = N\rho_b^n(t_h)$

13           $Uns_b(t_h) = N_b(t_h) - N_b^n(t_h)$

14   Calculate $P_b(t_h)$ till false

15   **end**

16   **else**

17   parameters remain unchanged

18   **end**

19   **end**

20   **end**

---

model. The RNC is a physical entity connected with all the networked BSs via backhaul links. At each hour the BSs send network information, such as, user density and BS battery level, to the RNC via special control signals. The proposed CCA model involves the RNC in adjusting the cell coverage areas of the BSs based on the network information, so as to address the traffic-energy imbalance in the network.

The proposed CCA based model follows the conventional WCA model and is presented in Algorithm 3. The CCA model also returns the number of users who are unable to be served $Uns_b(t_h)$ by BS b at hour t_h, the modified BSs coverage radius $R_b^n(t_h)$, the BS transmit power levels $P_b(t_h)$, and the new hourly number of users being served $N_b^n(t_h)$ by BS b as output.

A scenario may arise in the WCA model with a BS b being unable to serve all its associated users (Step 4) in an hour t_h due to the skewed traffic. In that case the adjacent BSs $(w \in \text{adj}_b)$ to BS b, being energy-surplus and low on traffic expand their coverage area by ϵ (Step 9) and try to accommodate the users being unserved $Uns_b(t_h)$ by BS b. Here adj_b denotes an adjacent matrix comprising of the indices of the adjacent BSs $(w \in \text{adj}_b)$ to each BS b. The users accommodated by the neighboring BS w is stored in $\text{served}_w(t_h)$ (Step 12), and the modified number of users being served by adjacent BS w, $N_w^n(t_h)$ is computed in Step 13. The users $u \in Uns_b(t_h)$ are associated with a BS $w \in adj_b$ from which it receives the best signal interference to noise ratio. It is notable that the adjacent BSs are also constrained by the peak power constraint (27). The network users still left unserved even after the proposed CCA are stored $Uns_b(t_h)$ in Step 23. Denoting f_{CCA} as the per-day frequency of coverage adjustment, the worst case time complexity for the proposed CCA model comes to be $O(f_{CCA} \times B^2 \times \Lambda)$, with value of Λ for various traffic skewness given in Table II. The default value of f_{CCA} for the proposed CCA model is 24 (i.e., it is done on an hourly basis). The values of f_{CCA} have been varied to observe the effect of the operator's revenue on frequency

Algorithm 3: Cooperative coverage adjustment (CCA) based strategy

---

Result: $Uns_b(t_h), P_b(t_h), R_b^n(t_h), N_b^n(t_h)$

1 After the WCA algorithm (Algorithm 2)
2 **for** $t_h \in f_{CCA}$ **do**
3   **for** $b = \{1, 2, \cdots, B\}$ **do**
4   **if** $Uns_b(t_h) != 0$ **then**
5   **for** $w = \{1, 2, \cdots, B\}$ **do**
6   **if** $w \in adj_b$ **then**
7   **while** $P_w(t_h) \leq P_{max}$ **do**
8   **if** $\Delta R_w(t_h) \leq \Delta R_b(t_h)$ **then**
9               $R_w^n(t_h) = R_w^n(t_h) + \epsilon$
10               $\Delta R_w(t_h) = R_w^n(t_h) - R_w(t_h)$
11   update $N_b(t_h)$ and get $\rho_b(t_h)$
12   update $served_w(t_h)$
13               $N_w^n(t_h) = N_w(t_h) + served_w(t_h)$
               further $\rho_w^n(t_h) = N_w^n(t_h)/\mathcal{U}$
14   Calculate $P_w(t_h)$ till false
15   **else**
16   exit
17   **end**
18   **end**
19   **else**
20   parameters unchanged
21   **end**
22   **end**
23       $Uns_b(t_h) = Uns_b(t_h) - \sum_w served_w(t_h)$
24   **else**
25   parameters unchanged
26   **end**
27   **end**
28 **end**

Table II: Iterations needed to converge at various traffic skewness levels

Traffic skewness levels $\longrightarrow$	17%	30%	50%	60%	70%	80%
WCA strategy	5	76	103	125	142	155
CCA strategy	7	81	111	127	144	160

of coverage adjustment.

From both the conventional WCA and the proposed CCA models, we obtain the number of users $N_b^n(t_h)$ being served by BS b at hour t_h for a given traffic skewness level. The value $N_b^n(t_h)$ is also the algorithmic solution for the optimum number users being hourly served by the BSs in the formulated revenue maximization problem (33) and is used to compute the value of R_{serv}. The BSs transmit power levels $P_b(t_h)$ obtained from the conventional WCA and proposed CCA model is used to compute the net energy consumed by BS b at hour t_h, given by $E_b(t_h) = (P_0 + P_b(t_h))$. $E_b(t_h)$ will be further used to compute the amount of surplus or deficient energy required by the operator, as discussed in the following sub-section.

C. Green energy allocation

After fixing the load on BSs using the WCA or CCA algorithm, we calculate the optimal energy demand, i.e., the corresponding excess energy that can be sold, or insufficient energy to generate OPEX. The hourly net energy consumed $E_b(t_h)$ by the BS b is used along with the hourly energy harvested $H_b(t_h)$ to compute the hourly amount of excess $E_b^S(t_h)$ or deficient $E_b^d(t_h)$ energy. These algorithmically computed energy values, $E_b^S = \sum_{t_h=1}^{24} E_b^S(t_h)$ and $E_b^d = \sum_{t_h=1}^{24} E_b^d(t_h)$, are used to calculate R_{sell} and OPEX discussed earlier in Section IV-A.

The green energy allocation algorithm is presented in Al-

Algorithm 4: Green energy allocation

Result: E_b^d, E_b^S

1 Input: $H_b(t_h), \beta^{cr}, \beta^{max}, E_b(t_h)$
2 Initialize: $\beta_{ini}^b, E_b^S = 0, E_b^d = 0, \beta_b(t_h) = 0, t_h = 1$
3 **for** $b = \{1, 2, \cdots, B\}$ **do**
4   $E_b^{bud} = \beta_b^{ini} - \beta^{cr} + \sum_{t_h=1}^{24} H_b(t_h)$
5   **for** $t_h = \{1, 2, \cdots, 24\}$ **do**
6     $\beta_b(t_h) = \beta_b(t_h - 1) + H_b(t_h) - E_b(t_h)$
7   **if** $\beta_b(t_h) \geq \beta^{max}$ **then**
8       $E_b^S = E_b^S + \beta_b(t_h) - \beta^{max}$ and $\beta_b(t_h) = \beta^{max}$
9   **else if** $\beta_b(t_h) \leq \beta^{cr}$ **then**
10       $E_b^d = E_b^d + \beta^{cr} - \beta_b(t_h)$ and $\beta_b(t_h) = \beta^{cr}$
11   **else**
12       $\beta_b(t_h) = \beta_b(t_h)$
13   **end**
14   **end**
15   $E_b^{bud} = E_b^{bud} - E_b^S$
16   **for** $t_h = \{1, 2, \cdots, 24\}$ **do**
17     $E_b^{alc}(t_h) = E_b^{bud} \frac{E_b(t_h)}{\sum_{t_h=0}^{24} E_b(t_h)}$
18   **end**
19 **end**

---

gorithm 4, where energy is allocated hourly to a BS b by its battery storage in accordance with the net hourly energy consumed $E_b(t_h)$ and the hourly energy harvested $H_b(t_h)$. Algorithm 4 returns the amount of energy which needs to be bought for BS b from the power-grid to avoid energy outage, E_b^d and the amount of energy which can be sold by BS b back to the power-grid, E_b^S.

The net green energy budget with BS b at the beginning of the day E_b^{bud} is given in Step 4, with β_b^{ini} being the initial battery level chosen randomly for each BS. The amount of surplus energy which can be sold back to the power-grid is calculated from Step 8, and the amount of deficient energy which needs to be purchased from the power-grid is calculated in Step 10. Finally, the energy being allocated to the BS in any hour is given in Step 17. In the following section we discuss the results obtained along with our observations and inferences.

V. RESULTS AND DISCUSSION

For simulation purpose and generation of results we consider the area under observation $A = 1\text{km}^2$ to be covered by six single operator BSs having $\lambda_u = 1800$. The dual powered BSs are enabled with 12 unit rated solar panels and 18 storage batteries in total. The corresponding CAPEX for the assumed solar dimensioning is computed to be 6998 USD. The system bandwidth BW is assumed to be 10 MHz with 512 subcarriers.

The values of parameters used in our analysis are as follows: AWGN noise variance $\sigma^2 = -150$ dBm/Hz, $P_{max} = 40$W, $\delta = 0.3$, $T_c = 27°C$ buffer length $B_Q = 100$ packets, $T_f = 10$ TTI, $T = 20000$ time slots, $t_w = 2T_f$, $p_0 = 0.9$, $P_0 = 118.7$ W, $\epsilon = 0.001$, $C_S = $ USD 1300\$ [37], $C_B = $ USD 216\$ [38], $\eta = 50\%$ and, $N_{bits} = 100$ bits/packet. We demonstrate the effects of traffic-energy imbalance on the user service and operator's revenue, when operating the dual-powered network through the conventional WCA and the proposed CCA strategies.
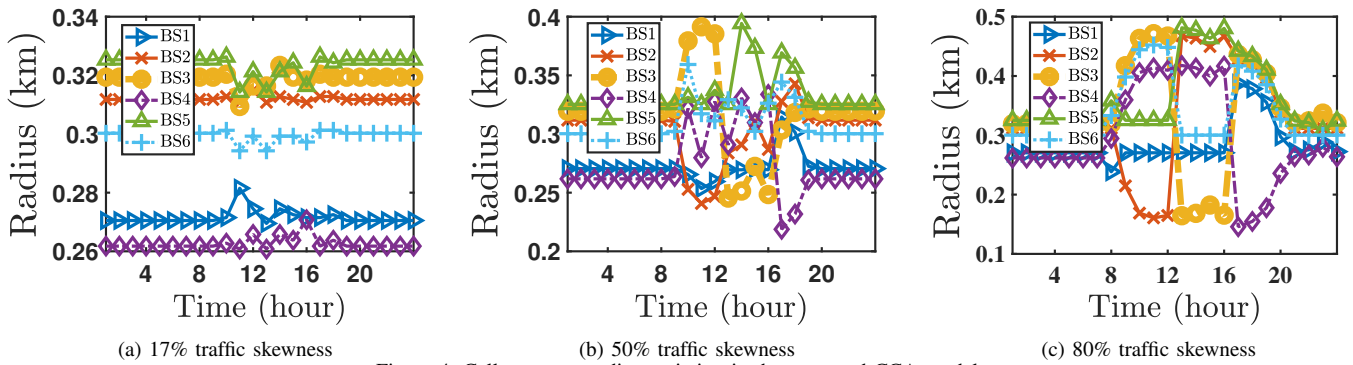
(a) 17% traffic skewness   (b) 50% traffic skewness   (c) 80% traffic skewness

Figure 4: Cell coverage radius variation in the proposed CCA model.

(a) WCA in 17% traffic skewness   (b) CCA in 17% traffic skewness   (c) WCA in 80% traffic skewness   (d) CCA in 80% traffic skewness
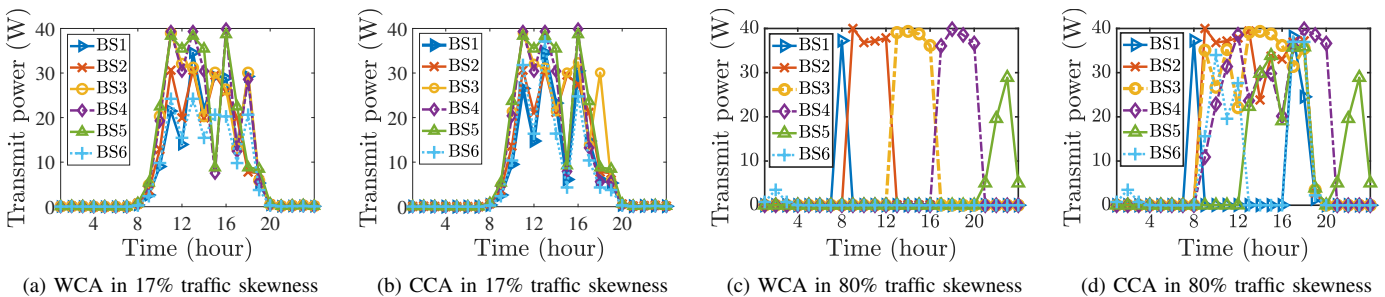
Figure 5: BS downlink transmit power variations at various traffic skewness levels.

A. Coverage radius and power variation

In this sub-section, we capture the effects of cooperative cell coverage adjustment through the proposed CCA approach on network performance in terms of user service.

We begin by demonstrating through Figs. 4(a) - 4(c), the BS cell radius variation observed under varying traffic skewness levels with the proposed CCA model. Adaptive cellular coverage in the proposed CCA model has been captured in terms of the mean and variance of the coverage radius variation. These trends are shown at all the considered traffic skewness levels in Table III. Fig. 4(a) shows the variation of cell radius when the BSs are subject to an average 17% traffic skewness. It is observed that the maximum mean and variance of the radius variation are 5×10^{-4} and 2×10^{-6} respectively at 17% skewed traffic skewness. When subjected to 80% traffic skewness (Fig. 4(c)), these values increase up to 0.0584 and 0.0078, respectively.

These results demonstrate the effective ways of network coverage level cooperation in the proposed CCA approach, resulting in much improved service guarantee to the users (Table III). In particular from Table III it is inferred that, while the network performance in terms of serving users degrades with increasing traffic skewness, the proposed CCA model increasingly outperforms the conventional WCA at higher traffic skewness levels. For instance, at 17% traffic skewness, both the conventional WCA and the proposed CCA are able to serve approximately 97% of the users on average. However, at a very high traffic skewness (80%), the conventional WCA model serves on average 70.61% of users, while the proposed CCA model serves 94.74% of the users in the network, thus offering a 25% gain.

Remark 1. *It can be clearly inferred that cell radius variation is more pronounced at higher traffic skewness levels, while lower traffic skewness levels undergo minor radius variations.*

Figs. 5(a) through 5(d) show the transmit power usage variation with the conventional WCA and the proposed CCA model when the network is subjected to two extreme traffic skewness levels. Figs. 5(a) and 5(b) show that, when the traffic across the BSs are homogeneously distributed, WCA and the CCA models distribute radiated power almost identically. However, at a much higher traffic skewness, radiated power in the proposed CCA model is more distributed across the different BSs (Fig. 5(d)). In contrast, in the conventional WCA model, the lightly loaded BSs (BS1, BS5, and BS6) have nearly zero power radiation, whereas the highly loaded BSs (BS2, BS3, and BS4) radiate almost full power (Fig. 5(c)). As it will be presented later in Fig. 7(b), the resultant revenue earned by selling surplus power in the proposed CCA model is lesser than that in the WCA approach.

Remark 2. *We infer that, when the network operates via the WCA mode, the traffic-energy imbalance increases with increasing traffic skewness and degrades the network performance in terms of user service. We observe that the effects of traffic-energy imbalance can be mitigated at cellular level via the proposed CCA model, which improves the network performance significantly.*

B. QoS performance

In this sub-section, we discuss the variation in user QoS with respect to PLER when subjected to varying traffic skew-

Table III: Effect of cell coverage with the CCA strategy

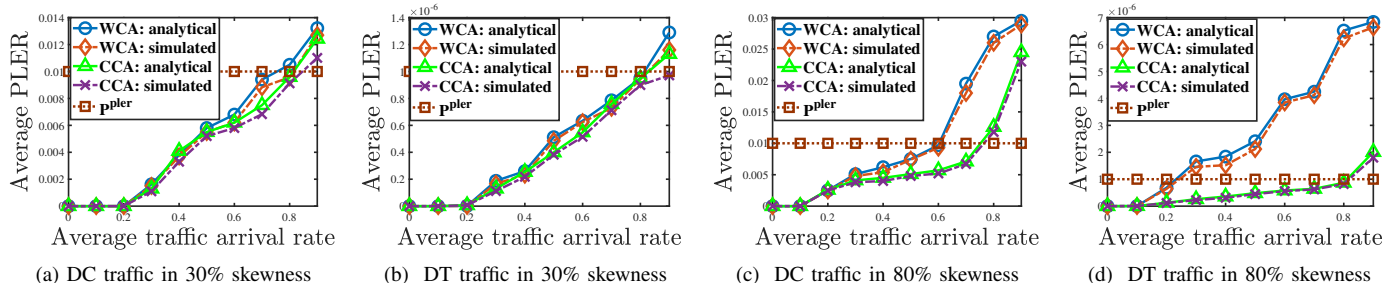| Traffic skewness levels ⟶	17%	30%	50%	60%	70%	80%
Maximum mean of radius variations (km)	5×10^{-4}	0.0212	0.0309	0.0477	0.0568	0.0584
Maximum variance of radius variations (km)	2×10^{-6}	9.93×10^{-4}	0.0032	0.0035	0.0052	0.0078
Fraction of users served without CCA	97.12%	93.44%	86.59%	81.77%	76.38%	70.61%
Fraction of users served with CCA	97.17%	95.29%	95.82%	94.95%	95.71%	94.74%

Figure 6: (a) - (b) PLER variation in DC and DT traffic at 30% traffic skewness without CCA and with CCA respectively, (c) - (d) PLER variation in DC and DT traffic at 80% traffic skewness without CCA and with CCA respectively.

ness. The 3GPP defined QoS specifications are given in Table I. Fig. 6 illustrates the variation of average PLER with respect to the average traffic arrival rate when the network is operated with the conventional WCA and with the proposed CCA model, in the presence of heterogeneous traffic. Through these plots we also verify the accuracy of the analytical modeling of PLER performance with respect to the simulation performance results. A good match is observed between the analytically obtained results and the simulated values. It is observed that the analytically obtained PLER performance is marginally poorer than that from the simulation. This difference is more prominent at higher traffic arrival rates. This is because, in the analysis, if the average delay of the packets exceeds the maximum delay upper bound, the entire set of packets in that window is dropped. On the contrary, in simulations, only the individual packets exceeding the delay upper bound are dropped. The effect of analytical approximation is poorer at higher traffic intensity because the system tends to operate at its limiting capacity. The corresponding root mean squared error (RMSE) values between the analytical and simulated values have also been computed.

Figs. 6(a) and 6(b) illustrate the PLER variation with respect to the average traffic arrival rate in the network for the delay-constrained and delay-tolerant traffic at 30% traffic skewness. Similarly, Figs. 6(c) and 6(d) showcase the PLER variation with respect to the average traffic arrival rate for both the traffic classes at 80% traffic skewness. It is inferred that PLER violation increases with increasing user traffic skewness and is more pronounced in the conventional WCA model. For instance, in the conventional WCA approach, analytical PLER for the delay-constrained traffic, rises to 1.32×10^{-2} at 30% traffic skewness in Fig. 6(a) and touches 2.95×10^{-2} at 80% traffic skewness in Fig. 6(c). The corresponding root mean squared error (RMSE) obtained between the analytical and simulated PLER values are 4.62×10^{-4} and 7.09×10^{-4}, respectively. When the network is operated with the proposed CCA model, these values reduce to about 1.12×10^{-2} in

Fig. 6(a) and 2.45×10^{-2} in Fig. 6(c). The corresponding RMSE values between the analytical and simulated values are 6.34×10^{-4} and 6.45×10^{-4}, respectively.

Remark 3. *It is inferred from these QoS plots, that the conventional WCA approach is prone to QoS guarantee violations while the proposed CCA approach offers significantly better QoS guarantee to the users in the network.*

C. Revenue analysis

Finally, we discuss the network performance in terms of the revenue metrics discussed in Section IV from the operator's perspective. The revenue metrics along with the net profit or revenue earned by the operator have been portrayed in Fig. 7. The net profit captured through these results is the solution of the formulated revenue maximization problem. The control signaling details and the associated overhead in the proposed CCA have not been considered in this study primarily because the information exchange for coverage adjustment is infrequent, e.g., once per hour or less. Moreover, the backhaul connectivity is typically through high capacity links, e.g., optical fiber connected, and hence capacity availability for data traffic exchange may not be affected by the additional infrequent coverage adjustment message exchanges.

Fig. 7(a) shows the operator's revenue earned by serving users (R_{serv}) subject to varying levels of traffic skewness under the considered network operation strategies. We clearly observe that the proposed CCA model outperforms the conventional WCA model in terms of revenue earned by serving users. The corresponding gain in R_{serv} obtained with the proposed CCA over the conventional WCA is given in Table IV. Through this trend we observe, that the operator obtains a gain up to 42.23% by serving users through the proposed CCA model at extreme 80% traffic skewness as compared to the conventional WCA.

Remark 4. *It is inferred that even though the revenue earned by the operator by serving users with either strategy decreases*

(a) User service revenue

(b) Energy selling revenue

(c) OPEX incurred

(d) Net revenue earned by operator

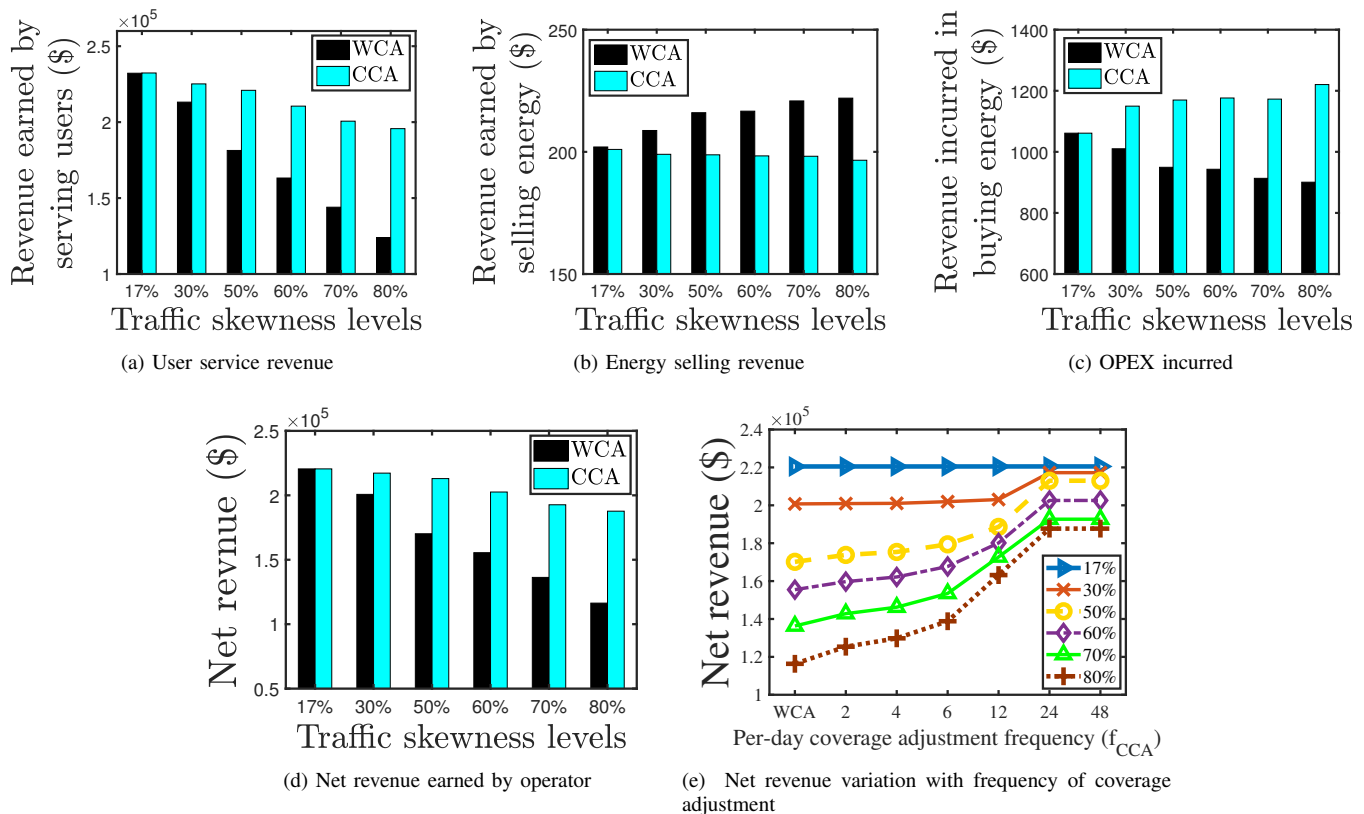(e) Net revenue variation with frequency of coverage adjustment

Figure 7: Annual variation of revenue metrics under various traffic skewness.

Table IV: Effects of cell coverage adjustment on the revenue metrics

Traffic skewness levels $\longrightarrow$	17%	30%	50%	60%	70%	80%
Gain in R_{serv} with CCA	0.06%	5.62%	21.82%	28.99%	39.33%	42.23%
Gain in R_{sell} with CCA	-0.49%	-4.67%	-7.98%	-8.45%	-10.25%	-11.45%
Gain in $OPEX$ with CCA	0%	13.82%	23.19%	24.74%	28.40%	35.49%
Gain in net revenue with CCA	0.006%	8.21%	25.15%	30.27%	41.34%	61.31%

as traffic skewness increases, the proposed CCA model earns consistently higher R_{serv} as compared to the WCA model. Thus demonstrating that the proposed CCA approach gives a better network performance in terms of serving users than the WCA, resulting in significant revenue gains.

Fig. 7(b) shows the operator's revenue earned through selling excess energy (R_{sell}) with a given solar dimensioning. We observe that in contrast to R_{serv}, the proposed CCA model obtains negative gain as compared with the conventional WCA model, as shown in Table IV. This can be justified intuitively, as the proposed CCA model tries to incorporate the edge users left over by the BSs affected with the skewed traffic, so as to bear a higher traffic load to the otherwise lower traffic experienced in the WCA model. This results in less excess energy being sold back to the power-grid and obtaining a negative gain up to 11.45% at 80% traffic skewness as shown in Table IV.

Remark 5. *It is inferred that in contrast to the revenue earned by serving users R_{serv}, the conventional WCA model consistently obtains higher gains for R_{sell} at all traffic skewness*

levels as compared to the proposed CCA model.

Fig. 7(c) showcases the plot for the OPEX incurred by the operator with the BSs subject to various traffic skewness levels. The corresponding gain in OPEX with the proposed CCA approach is shown in Table IV. We observe that the proposed CCA model incurs a higher OPEX of up to 35.49% at extreme 80% traffic skewness. This can be intuitively justified as the BSs serve more users in the proposed CCA model to address traffic imbalance. This results in a larger traffic load on the BSs, which otherwise would have been lightly loaded, resulting in more energy-deficient BSs and thus incurring larger OPEX.

Remark 6. *It is inferred that the proposed CCA model consistently incurs higher OPEX as compared to the traditional WCA model.*

Finally, the operator's net profit or revenue earned with varying traffic skewness levels for both the network operation strategies is shown in Fig. 7(d). The corresponding gain in net profit with the proposed CCA approach is shown in Table IV. It can be seen that the net profit is almost equal in both

the conventional WCA as well as the proposed CCA model for the lowest traffic skewness level of 17%. Further, it is observed that with increasing traffic skewness, while the net profit decreases with both strategies as seen from Fig. 7(d), the proposed CCA model gives a consistently higher profit value of up to 61.31% at extreme 80% traffic skewness as compared to the traditional WCA model.

The effects of varying the daily coverage adjustment frequency on the operator's net revenue are captured in Fig. 7(e). Since the proposed CCA model is observed to be a function of the per-day frequency of coverage adjustment f_{CCA}, the revenue variation is observed at different frequencies. Frequency of coverage adjustment also captures the complexity of the proposed CCA model. Hence, through Fig. 7(e) we portray the effect of varying the time complexity of the proposed CCA model on the operator revenue. $f_{CCA} = 24$ denotes the default hourly coverage adjustment, while $f_{CCA} = 48$ denotes an increased coverage adjustment frequency at every 30 minutes, and so on.

It is observed that reducing the frequency of coverage adjustment cycles does not affect the net revenue at 17% traffic skewness. On the contrary, lower frequencies of coverage adjustment result in substantial reduction of the net revenue for all other skewed traffic scenarios. It is also observed that the revenue at an increased coverage adjustment frequency of $f_{CCA} = 48$, is almost equal to that with $f_{CCA} = 24$. Thus, with the given hourly traffic profile, the considered default hourly coverage update frequency is noted to be nearly optimal in terms of net revenue. It is interesting to note that while the net revenue reduces with lowering adjustment frequency, the revenue earned is still substantially higher than the revenue obtained via the WCA model.

Remark 7. *These results demonstrate the dominance of revenue earned by serving users R_{serv} over other revenue metrics. This is because, even though the proposed CCA model leads to lower revenue through selling energy R_{sell} and incurs higher OPEX, still the net profit earned by proposed CCA is way higher than that earned by WCA at all traffic skewness levels. Thus showing the importance of addressing traffic-energy imbalance at cellular level.*

VI. CONCLUSION

The paper has studied the impact of cooperative cellular coverage adjustment on the network performance in a cellular network with dual-powered BSs. The developed analytical framework has captured the network performance in terms of average number of users served and revenue earned by the operator while fulfilling the heterogeneous QoS requirements of the users. In the proposed approach the RNC invokes adjustment of cell coverage areas based on traffic density and energy availability within the individual BSs. The formulated revenue maximization problem accounts for QoS guarantee to users, OFDM based resource allocation, stochasticity in user traffic, harvested energy, and the channel variations.

The proposed cellular coverage adjustment based approach has been compared with the conventional without coverage adjustment approach. In presence of skewed user traffic,

the conventional approach has been found relatively poorer compared to that in the proposed coverage adjustment based approach, in terms of average users served and the operator revenue earned. The results demonstrate that the efficacy of the proposed coverage adjustment model is more pronounced with the increased skewness of traffic intensity. It is also inferred that, while reducing the coverage adjustment frequency overhead leads to substantial reduction in revenue gain, it is still significantly higher than that obtained without coverage adjustment. In addition to cost incentives for network operators, the study is expected to pave the way to advance green energy solutions in cellular communications, thereby aiding in reduction of carbon energy footprint.

REFERENCES

[1] A. Balakrishnan, S. De, and L. C. Wang, "Traffic skewness-aware performance analysis of dual-powered green cellular networks," in *Proc. IEEE GLOBECOM, Taipei, Taiwan*, Dec. 2020, pp. 1–6.

[2] B. K. J. Al-Shammari, N. Al-Aboody, and H. S. Al-Raweshidy, "IoT traffic management and integration in the QoS Supported network," *IEEE Internet Things J.*, vol. 5, no. 1, pp. 352–370, 2018.

[3] M. A. Marsan, G. Bucalo, A. Di Caro, M. Meo, and Y. Zhang, "Towards zero grid electricity networking: Powering BSs with renewable energy sources," in *Proc. IEEE ICC Wksp., Budapest, Hungary*, June 2013.

[4] E. Oh, B. Krishnamachari, X. Liu, and Z. Niu, "Toward dynamic energy-efficient operation of cellular network infrastructure," *IEEE Commun. Mag.*, vol. 49, no. 6, pp. 56–61, 2011.

[5] H. Jo, Y. J. Sang, P. Xia, and J. G. Andrews, "Heterogeneous cellular networks with flexible cell association: A comprehensive downlink SINR analysis," *IEEE Trans. Wireless Commun.*, vol. 11, no. 10, pp. 3484–3495, 2012.

[6] L. Chettri and R. Bera, "A Comprehensive Survey on Internet of things (IoT) toward 5G wireless systems," *IEEE Internet Things J.*, vol. 7, no. 1, pp. 16–32, 2020.

[7] Z. Hasan, H. Boostanimehr, and V. K. Bhargava, "Green cellular networks: A survey, some research issues and challenges," *IEEE Commun. Surveys Tuts.*, vol. 13, no. 4, pp. 524–540, 2011.

[8] S. Suman and S. De, "Low complexity dimensioning of sustainable solar-enabled systems: A case of base station," *IEEE Trans. Sustain. Comput.*, pp. 1–1, 2019.

[9] X. Liu and N. Ansari, "Dual-battery enabled profit driven user association in green heterogeneous cellular networks," *IEEE Trans. Green Commun. Netw.*, vol. 2, no. 4, pp. 1002–1011, 2018.

[10] H. Wu, C. Qiao, S. De, and O. Tonguz, "Integrated cellular and ad hoc relay systems: iCAR," *IEEE J. Sel. Areas in Commun.*, vol. 19, no. 10, pp. 2105–2115, Oct. 2001.

[11] A. Goldsmith and S. Wicker, "Design challenges for energy-constrained ad hoc wireless networks," *IEEE Wireless Commun.*, vol. 9, no. 4, pp. 8–27, 2002.

[12] E. Oh, K. Son, and B. Krishnamachari, "Dynamic Base Station Switching-On/Off strategies for green cellular Networks," *IEEE Trans. Wireless Commun.*, vol. 12, no. 5, pp. 2126–2136, 2013.

[13] D. Renga, H. Al Haj Hassan, M. Meo, and L. Nuaymi, "Energy management and base station On/Off switching in green mobile networks for offering ancillary services," *IEEE Trans. Green Commun. Netw.*, vol. 2, no. 3, pp. 868–880, 2018.

[14] Z. Niu, Y. Wu, J. Gong, and Z. Yang, "Cell zooming for cost-efficient green cellular networks," *IEEE Commun. Mag.*, vol. 48, no. 11, pp. 74–79, 2010.

[15] S. Hu, X. Chen, W. Ni, X. Wang, and E. Hossain, "Modeling and Analysis of energy harvesting and smart grid-powered wireless communication networks: A contemporary survey," *IEEE Trans. Green Commun. Netw.*, vol. 4, pp. 461–496, 2020.

[16] J. Wang, C. Jiang, Z. Han, Y. Ren, and L. Hanzo, "Network Association strategies for an energy harvesting aided super-WiFi network relying on

measured solar activity," *IEEE J. Sel. Areas Commun.*, vol. 34, no. 12, pp. 3785–3797, 2016.

[17] H. Al Haj Hassan, D. Renga, M. Meo, and L. Nuaymi, "A novel energy model for renewable energy-enabled cellular networks providing ancillary services to the smart grid," *IEEE Trans. Green Commun. Netw.*, vol. 3, pp. 381–396, 2019.

[18] S. Suman and S. De, "Solar-enabled green base stations: Cost versus utility," in *Proc. IEEE WoWMoM, Macau, China*, June 2017, pp. 1–8.

[19] V. Chamola, B. Krishnamachari, and B. Sikdar, "Green energy and delay aware downlink power control and user association for off-grid solar-powered base stations," *IEEE Syst. J.*, vol. 12, no. 3, pp. 2622–2633, 2018.

[20] H. Al Haj , K. Deep Singh, and L. Nuaymi, "Grid energy consumption of mixed-traffic cellular networks with renewable energy sources," in *Proc. IEEE OnlineGreenComm, Piscataway, NJ, USA*, Nov. 2016, pp. 1–6.

[21] Li Chen, Bin Wang, X. Chen, Xin Zhang, and Dacheng Yang, "Utility-based resource allocation for mixed traffic in wireless networks," in *Proc IEEE INFOCOM Wkshps., Shanghai, China*, Apr. 2011, pp. 91–96.

[22] L. Xiang, X. Ge, C.-X. Wang, F. Y. Li, and F. Reichert, "Energy efficiency evaluation of cellular networks based on spatial distributions of traffic load and power consumption," *IEEE Trans. Wireless Commun.*, vol. 12, no. 3, pp. 961–973, 2013.

[23] X. Chen, J. Wu, Y. Cai, H. Zhang, and T. Chen, "Energy-efficiency oriented traffic offloading in wireless networks: A brief survey and a learning approach for heterogeneous cellular networks," *IEEE J. Sel. Areas in Commun.*, vol. 33, no. 4, pp. 627–640, 2015.

[24] D. Lee, S. Zhou, X. Zhong, Z. Niu, X. Zhou, and H. Zhang, "Spatial modeling of the traffic density in cellular networks," *IEEE Wireless Commun.*, vol. 21, no. 1, pp. 80–88, 2014.

[25] J. Wu, S. Zhou, and Z. Niu, "Traffic-aware base station sleeping control and power matching for energy-delay tradeoffs in green cellular networks," *IEEE Trans. Wireless Commun.*, vol. 12, no. 8, pp. 4196–4209, 2013.

[26] 3GPP: A global initiative. [Online]. Available: https://www.3gpp.org/specifications

[27] Yi Zhang, L. Budzisz, M. Meo, A. Conte, I. Haratcherev, G. Koutitas, L. Tassiulas, M. A. Marsan, and S. Lambert, "An overview of energy-efficient base station management techniques," in *Proc. IEEE TIWDC, Genoa, Italy*, 2013, pp. 1–6.

[28] System advisor model: National renewable energy laboratory. [Online]. Available: https://www.sam.nrel.gov

[29] B. Al-Manthari, N. Nasser, and H. Hassanein, "Downlink scheduling with economic considerations for future wireless networks," *IEEE Trans. Veh. Tech.*, vol. 58, no. 2, pp. 824–835, 2009.

[30] D. P. Bertsekas, R. G. Gallager, and P. Humblet, *Data Networks*. Prentice-Hall International New Jersey, 1992, vol. 2.

[31] J. Jang and K. B. Lee, "Transmit power adaptation for multiuser ofdm systems," *IEEE J. Sel. Areas in Commun.*, vol. 21, no. 2, pp. 171–178, 2003.

[32] M. Abramowitz, I. A. Stegun, and R. H. Romer, "Handbook of Mathematical Functions with Formulas, Graphs, and Mathematical Tables," 1988.

[33] What will happen to solar panels after their useful lives are over? [Online]. Available: https://www.greenbiz.com

[34] True cost of providing energy to telecomm towers in India. [Online]. Available: https://www.gsma.com

[35] Economic times-falling solar power cost lead to pricing disputes. Nov. 2009. [Online]. Available: https://economictimes.indiatimes.com

[36] Antennae location methodology for a telecomm operator in India, IIM-B, Working paper no. 454. [Online]. Available: https://www.iimb.ac.in

[37] Economic Times-Solar Panel Cost: Price range of different types of solar panels and how much govt. subsidy you can avail for installing one. May 2014. [Online]. Available: https://economictimes.indiatimes.com

[38] Batteries for solar systems-Renewable Energy Batteries. [Online]. Available: https://www.thesolarbiz.com/batteries.html

Ashutosh Balakrishnan (S'16) received the Bachelor of Technology (B. Tech) degree in Electronics and Telecommunication Engineering from National Institute of Technology Raipur, India in 2019. He is currently pursuing his direct Ph. D. degree from Department of Electrical Engineering, Indian Institute of Technology Delhi, India, under IIT Delhi – NYCU Taiwan Joint Doctoral Program. His research interests include energy harvesting enabled wireless communication networks, green communication, and cross-layer design.

Swades De (S'02 – M'04 – SM'14) received the B.Tech. degree in Radiophysics and Electronics from the University of Calcutta in 1993, the M.Tech. degree in Optoelectronics and Optical Communication from IIT Delhi in 1998, and the Ph.D. degree in Electrical Engineering from the State University of New York at Buffalo in 2004.

Dr. De is currently a Professor with the Department of Electrical Engineering, IIT Delhi. Before moving to IIT Delhi in 2007, he was a Tenure-Track Assistant Professor with the Department of ECE, New Jersey Institute of Technology, Newark, NJ, USA, from 2004–2007. He worked as an ERCIM Post-doctoral Researcher at ISTI-CNR, Pisa, Italy (2004), and has nearly five years of industry experience in India on telecom hardware and software development, from 1993–1997, 1999. His research interests are broadly in communication networks, with emphasis on performance modeling and analysis. Current directions include energy harvesting wireless networks, broadband wireless access and routing, network coexistence, smart grid networks, and IoT communications. Dr. De currently serves as an Area Editor of IEEE COMMUNICATIONS LETTERS and Elsevier Computer Communications, and an Associate Editor of IEEE TRANSACTIONS ON VEHICULAR TECHNOLOGY and IEEE WIRELESS COMMUNICATIONS LETTERS.

Li-Chun Wang (M'96 – SM'06 – F'11) received Ph. D. degree from the Georgia Institute of Technology, Atlanta, in 1996. From 1996 to 2000, he worked at AT&T Laboratories, where he was a Senior Technical Staff Member in the Wireless Communications Research Department. Since August 2000, he has joined the Department of Electrical and Computer Engineering at National Yang Ming Chiao Tung University in Taiwan. He is now a Chair Professor and is jointly appointed by the Department of Computer Science and Information Engineering from the same university.

Dr. Wang was elected to an IEEE Fellow in 2011 for his contributions to cellular architecture and radio resource management in wireless networks. He has won two Distinguished Research Awards from Taiwan's Ministry of Science and Technology (2012, 2017). He was the co-recipients of IEEE Communications Society Asia-Pacific Board Best Award (2015), Y. Z. Hsu Scientific Paper Award (2013), and IEEE Jack Neubauer Best Paper Award (1997).

His recent research interests are in the areas of cross-layer optimization for wireless systems, data-driven radio resource management, software-defined heterogeneous mobile networks, big data analysis for industrial Internet of things, and AI-enabled unmanned aerial vehicular (UAV) networks. He holds 26 US patents, and has published over 300 journal and conference papers, and co-edited the book, "Key Technologies for 5G Wireless Systems," (Cambridge University Press 2017).